Eur. Phys. J. D **4**, 309–319 (1998)

THE EUROPEAN PHYSICAL JOURNAL D

Dissociative excitation of the fluoromethanes by electron impact

O. Keller[a], C. Mang, M. Nikola, and G. Schulz

Fachbereich Experimentalphysik, Universität des Saarlandes, 66041 Saarbrücken, Germany

Received: 25 February 1998 / Revised: 29 May 1998 and 18 June 1998 / Accepted: 23 June 1998

Abstract. Emission spectra following electron impact on molecules of the homologous series of fluoromethanes CH_xF_{4-x} with $x = 0-4$ have been investigated from the near infrared at 700 nm to the ultraviolet VUV-spectral region at 100 nm. Earlier experimental data for the visible and ultraviolet spectral region were revised and evaluated again on the basis of reliable new data for the dynamic viscosity of the molecules. The measurement of absolute and relative cross-sections were systematically extended into the VUV region from 100 nm to 200 nm. The examination of atomic lines as well as molecular band systems in the VUV gives further insight into the dissociation mechanism and shows that many excited levels even of atomic and molecular species cannot be populated directly, but only by transitions from higher-lying energy levels. Simple steric effects can be distinguished from more complex transition phenomena.

PACS. 34.80.Gs Molecular excitation and ionization by electron impact – 52.20.Fs Electron collisions

1 Introduction

The dissociation of fluoromethanes following electron impact has been the subject of many investigations in the past. In an earlier paper [3] we discussed systematically the emission spectra of CH_3F, CH_2F_2 and CHF_3. Now absolute emission cross-sections of the diatomic band systems of CH and CH^+ are calculated for all H-containing compounds on the basis of synthetic spectra. With data for the dynamic viscosity of the fluoromethanes taken from literature absolute emission cross-section values which we reported earlier have to be corrected.

Using a new VUV-apparatus the investigations were extended into the spectral region from 100 nm to 200 nm, where several spectral lines of atomic H and C are found. An analysis of these atomic lines may be helpful to determine dissociation channels which lead to the total dissociation of the target compound into atomic fragments. Absolute emission cross-sections of atomic lines in the VUV spectral region could be calculated relative to known cross-section values of atomic lines and diatomic band systems of reference gases as CH_4 and N_2.

We also examined the emission spectrum of CF_4, especially the continuous emission in the VUV-spectrum of CF_4 between 150 nm and 180 nm in comparison to the continuous emission in the ultraviolet and visible spectral region between 200 nm and 500 nm. Comparing the excitation functions of both continua, the radiative species can be identified which will be formed immediately after the collision process.

[a] e-mail: okeller@rz.uni-sb.de

2 Experimental

For the investigation of optical emission spectra and the measurement of absolute and relative emission cross-sections two different experimental setups have been used, a gas-target-system and a crossed-beam-system which both have been described in detail earlier [1–3]. Both systems could be inserted into the IRUV-apparatus which allowed investigations in the spectral range from 200 nm to 800 nm. In addition to the head-on-photomultiplier (Hamamatsu R1104) now a side-on-photomultiplier (Hamamatsu R1527P) with maximum sensitivity at 420 nm and a dark count rate of only 5 cps has been used.

The measurements in the region from 100 nm to 200 nm were performed with a UHV-recipient directly coupled to a vacuum-monochromator. In order to avoid contamination of the the large volume of the monochromator by the target gases or by air, if the electron gun has to be changed, both components were separated by a MgF_2-window as shown in Figure 1. The radiation from the interaction region was focussed by a MgF_2-coated mirror onto the entrance slit of a 0.75 m monochromator. The emitted light was analyzed by a standard photon counting system using a solar blind photomultiplier (Hamamatsu R1259P) with maximum efficiency at a wavelength of 120 nm and a dark count rate below one count per second. Because of the special optical setup in the VUV-apparatus, only the crossed-beam-system could be used in the VUV-spectral region. The entire apparatus and the data requisition and analysis were controlled by programmable microprocessor devices.

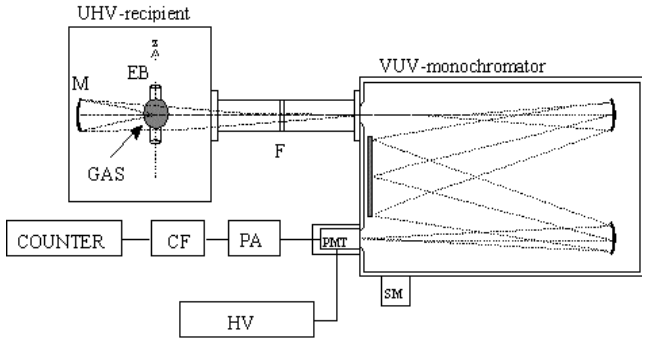

Fig. 1. VUV-apparatus, UHV-recipient and 0,75 m vacuum monochromator, EB electron beam, Gas molecular beam, M mirror, F MgF_2-window, PMT photomultipliertube, PA preamplifier, CF constant fraction discriminator, counter, SM stepping motor, HV high voltage supply.

3 Calibration of the electron energy and the spectral sensitivity of the optical detection system

In the IRUV-apparatus the calibration of the electron energy was performed relative to the thresholds of the excitation functions of the molecular nitrogen bands at 337.1 nm and 391.4 nm as described earlier [3]. For energy calibration purposes in the VUV region we used the threshold at 8.44 eV of the excitation function of the xenon resonance line at 146.9 nm which was determined before each one of the fluoromethanes measurements.

The spectral sensitivity of the optical detection system in the IRUV-apparatus was determined relative to the emission of a calibrated tungsten iodine lamp, as described earlier [3]. In order to obtain absolute emission cross-sections, the spectral intensities have to be normalized to the electron current and to the density of the target molecules in the interaction region as a function of temperature and gas pressure in the gas-target-system. The pressure was measured by a spinning rotor gauge (MKS Instruments SRG-2). The reliability of the monitored gas pressure depends strongly on the parameters of the spinning rotor gauge. In earlier investigations we used the temperature dependent dynamic viscosity values of CH_4 and calculated dynamic viscosity values for CF_4. The data for CH_3F, CH_2F_2 and CHF_3 were obtained by a linear fit between the values for CH_4 and CF_4. But measuring the gas pressure of the target gases before and behind the multicapillary orifice used for reducing the pressure and comparing them with known species under molecular flow condition, we saw, that the calculated viscosity data must be erroneous. With data from literature for the dynamic viscosities [4] we find different values for the density of the target molecules. As a consequence, different gas dependent correction factors must be used for the calculation of absolute emission cross-sections. The reliability of the dynamic viscosity data could be verified by comparing the gas pressure in the interaction region and the gas pressure before the multicapillary orifice. The ratio of both values is plotted versus the gas pressure before the multicapillary orifice in Figure 2 for several gases. These values vary only within a very small range of $\pm$ 0.9% which is less than the accuracy of the spinning rotor gauge of $\pm$ 1.5%. Therefore we assumed the same value for all gases under molecular flow conditions. The values of absolute emission cross-sections which were reported earlier [3] and which have to be corrected are now assigned by an asterix in Tables 3.

In the VUV-spectral region absolute emission cross-section could only be determined by comparison with known absolute emission cross-sections of other atomic or molecular species with an appropriate emission in the same spectral region. For the absolute emission cross-section of an atomic line, *i.e.* of a reference gas, one finds:

$$\sigma_{ref} = \frac{\alpha(T)}{E(\lambda_0)} Z_{ref} \tag{1}$$

where σ_{ref} is the absolute emission cross-section at a given electron energy, $\alpha(T)$ a temperature depending factor which contains the density of target molecules within the molecular beam for given experimental conditions, $E(\lambda_0)$ is the sensitivity of the entire optical detection system at the wavelength λ_0 and Z_{ref} the sum of the measured count rates.

In the spectral range between 120 nm and 260 nm absolute emission cross-sections of atomic lines and molecular band systems have been reported by various authors [5–9]. The band systems and atomic lines which could be used for calibration purposes are the following:

- the 4th positive system of CO, $A^1\Pi \rightarrow X^2\Sigma$, in a spectral range between 134.8 nm and 198.8 nm following 300 eV electron impact [5,9];
- the Lyman-Birge-Hopfield-system (LBH) of N_2, $a^1\Pi_g \rightarrow X^1\Sigma_g^+$, in a spectral range between 134.8 nm and 198.8 nm following 300 eV electron impact;
- the Lyman-α-line at 121.6 nm following 100 eV electron impact on CH_4 [6];
- two strong atomic N-lines at 174.4 nm and 149.4 nm following 300 eV electron impact on N_2.

Emission spectra following electron impact on N_2, CO and CH_4 were measured in order to determine the response of the apparatus. Subsequently the fluoromethanes were measured under the same experimental conditions. The gas pressure before the multichannel orifice was kept constant to within $\pm$ 0.5% by means of a gas flow control valve. As the molecular gas flow through the multichannel orifice varied only by 1%, when the target gas was changed, it was justified to assume equal experimental conditions in the molecular beams simply by keeping constant the gas pressure in the volume before the multichannel orifice.

For the emission spectrum of N_2, the most prominent features are atomic lines. The LBH-system is unsuitable for calibration purposes due to the long lifetime of the emitting states [10–12]. The emission spectrum of CO shows diatomic molecular bands of the 4th positive system as well as several atomic lines. Table 1 shows the identified molecular bands and absolute emission cross-sections reported by other authors [4,8]. The (1–1)-band

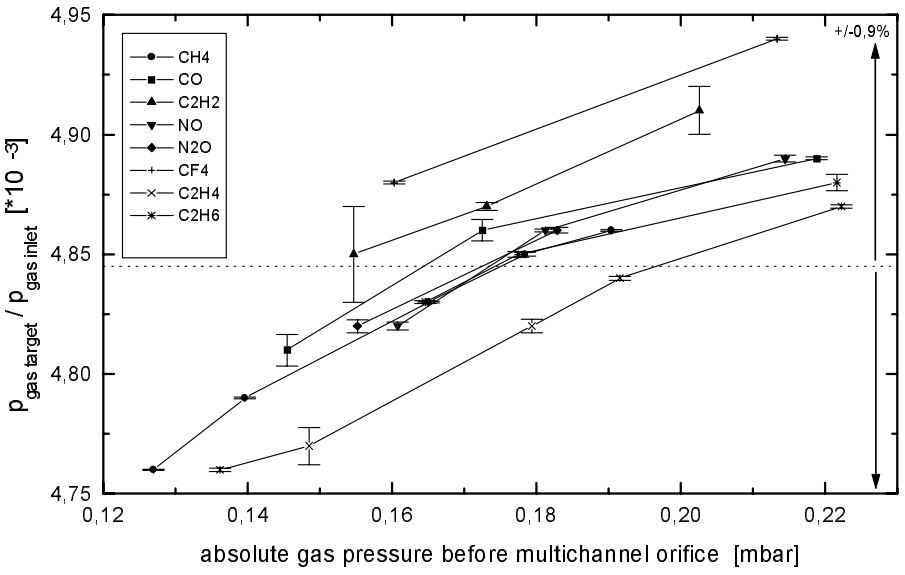

Fig. 2. The relation of the gas pressure in the reaction region to the gas pressure before the multicapillary orifice as function of the absolute gas pressure.

at 156.0 nm is superimposed on an atomic C-line and was not used, the (3–4)-band is very close to an atomic C-line and could not be resolved, given the spectral resolution. The absolute emission cross-section of the Lyman-α-line at 126.1 nm following electron impact on CH_4, reported by Möhlmann and de Heer [8] with a value of 11×10^{-18} cm^2 could be used for calibration purposes without any restrictions.

4 Results

4.1 Emission spectra and absolute emission cross-sections

The emission spectra following 100 eV electron impact in the spectral region between 200 nm and 800 nm have been described earlier [3]. The identification of diatomic spectral components and the calculation of absolute emission cross-sections have been performed using synthetic spectra of the $A^2\Delta \rightarrow X^2\Pi$-system of CH. But because the $A^2\Delta \rightarrow X^2\Pi$-system of CH is contaminated by the $A^1\Pi \rightarrow X^1\Sigma^+$-system of CH^+, it was necessary to add a synthetic spectrum of this system in order to achieve maximum precision for the resulting cross-section values. As one observers only one P-, J- and Q-branch in the emission spectrum, it was not necessary to distinguish between Hund's coupling cases a and b for the $^1\Pi \rightarrow {}^1\Sigma$-transitions and, therefore, the calculation of rotational term values was performed using a simple power series. The corresponding Hönl-London-factors were taken from Herzberg [13]. Appropriate molecular constants were reported by Herzberg [13], Carrington and Ramsey [14] and Mahan and O'Keefe [15]. Finally, synthetic spectra for the $B^2\Sigma \rightarrow X^2\Pi$-system of CH at 350 nm were calculated in the same way. The $^2\Sigma \rightarrow {}^2\Pi$-system shows the same transitions as the $^2\Pi \rightarrow {}^2\Sigma$-system. It is only for large separation between $^2\Pi_{1/2}$ and $^2\Pi_{3/2}$, that one observes two subbands $^2\Sigma \rightarrow {}^2\Pi_{1/2}$ and $^2\Sigma \rightarrow {}^2\Pi_{3/2}$ and, therefore, two components for the P-, Q- and R-branches must be considered. Termvalues for the $X^2\Pi$-state were calculated using the same formulas as for the $A^2\Delta \rightarrow X^2\Pi$-system. The term values for the $B^2\Sigma$-state were calculated with the formula of Herzberg. Hönl-London-factors for the $^2\Sigma \rightarrow {}^2\Pi$-transition were taken from Earls [16]. When no data for Franck-Condon-Factors of the considered vibrational transitions were available, the formulas given by Waldenstrom and Naqvi [17] could be used to calculate these factors. For small values of the vibronic quantum numbers ν' and ν'' they found an excellent agreement

Table 1. Identified vibronic bands of the CO: $A^1\Pi \rightarrow X^2\Sigma$-system. Absolute emission cross-section values following 300 eV electron impact onto CO are taken from the literature. All values have the unit 10^{-19} cm^2.

Wavelength (nm)	Vibronic transition ($\nu' \rightarrow \nu''$)	[5]	[7]
138.4	7–1	-	1.01
140.8	6–1	-	2.54
146.3	4–1	-	5.69
149.3	3–1	-	2.80
140.9	1–0	-	19.1
154.2	3–2	-	7.27
156.0	1–1	-	10.6
157.6	2–2	-	6.30
159.7	0–1	-	7.50
163.0	2–3	-	6.19
164.7	3–4	3.4	3.62
166.9	1–3	3.34	3.26
172.9	1–4	6.48	6.21
179.2	1–5	4.39	4.43

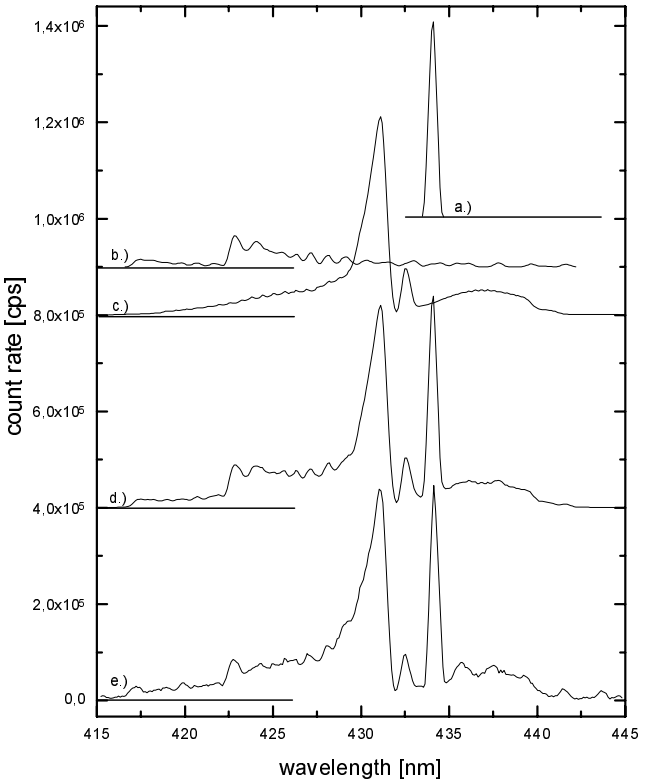

Fig. 3. Comparison of calculated and measured emission spectrum of CH_4, (a) convolution of H_γ-line with the apparatus-profile, (b) simulation of CH^+: $A_1\Pi \rightarrow X_1\Sigma^+$ system (0–0) and (2–1) band, $T_{rot} = 3000$ K, (c) simulation of CH: $A_2\Delta \rightarrow X_2\Pi$ system (0–0), (1–1) and (2–2) band, $T_{rot} = 3000$ K, (d) convolution of (a), (b) and (c), (e) measured emission spectrum. Horizontal lines indicate the corresponding zero-lines.

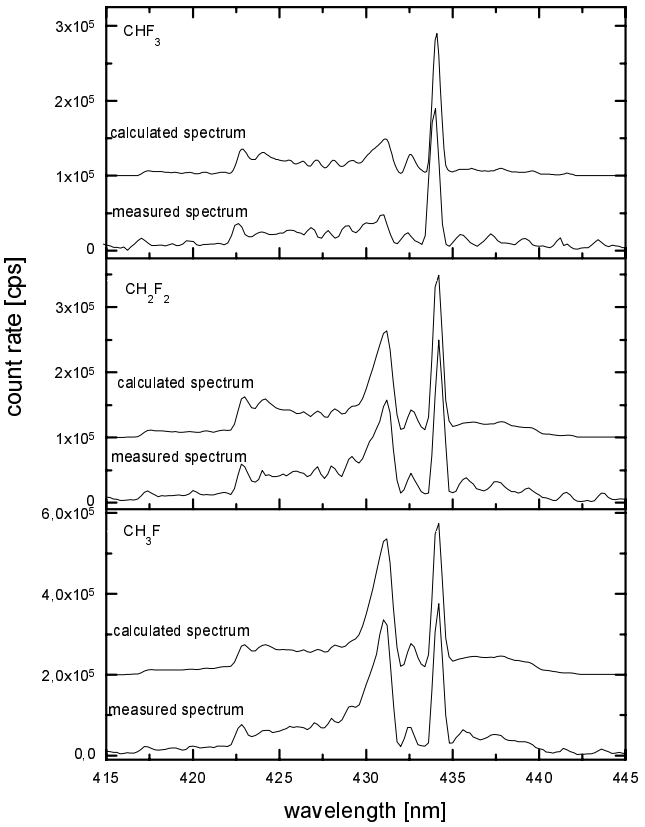

Fig. 4. Comparison of calculated and measured spectra for the various compounds.

between calculated and experimentally determined factors for vibrational transitions of N_2. A comparison of synthetic emission spectra of CH on the basis of calculated Franck-Condon-Factors with the intensity distribution of measured emission spectra showed that it was justified to use the formulas in our case too.

Synthetic spectra for the investigated diatomic band systems were at first calculated for the emission spectrum of CH_4 because the absolute emission cross-sections of the $A^2\Delta \rightarrow X^2\Pi$-system of CH_4 are well-known. Figures 3a–3e show the comparison between the calculated spectrum and the experimentally determined emission spectrum of CH_4. The $A^2\Delta \rightarrow X^2\Pi$-system of CH shows only parts of the (0–0)-, (1–1)- and (2–2)-bands in this spectral region, the $A^1\Pi \rightarrow X^1\Sigma^+$-system of CH^+ consists of the (0–0)- and the (2–1)-bands. The discrete bands in the emission spectrum above a wavelength of 435 nm are due to the (0–1)-band of the $B^2\Sigma \rightarrow X^2\Pi$-system of CH and were not considered in the calculations of the synthetic spectra. Absolute emission cross-sections for the considered band systems are listed in Table 2. The determined values show an excellent agreement with the data from literature [8,9]. The calculated spectra allow furthermore the determination of absolute emission cross-section values for single vibronic transitions. In the same manner, absolute emission cross-section values for CH_3F, CH_2F_2 and CHF_3 for the same systems were caculated from the synthetic spectra and listed in Table 3. The comparison between the calculated spectra and the measured emission spectra is shown in Figure 4. The values for the $A^2\Delta \rightarrow X^2\Pi$-system of CH show a strong dependence on the number of H- and F-atoms in the target, respectively, whereas the values for the $A^1\Pi \rightarrow X^1\Sigma^+$-system of CH^+ seem to be nearly unchanged for CH_3F and CH_2F_2.

Table 2. Absolute emission cross-section values following 100 eV electron impact onto CH_4 for the observed CH: $A^2\Delta \rightarrow X^2\Pi$-system and the CH^+: $A^1\Pi \rightarrow X^1\Sigma$-system in comparison with literature data. All values have the unit 10^{-19} cm^2.

Transition		[8]	[9]
CH: $A^2\Delta \rightarrow X^2\Pi$			
complete transition	17.6 ± 1.05	17.0	17.0
(0–0)	8.5 ± 0.51	-	-
(1–1)	7.4 ± 0.44	-	-
(2–2)	1.7 ± 0.10	-	-
CH^+: $A^1\Pi \rightarrow X^1\Sigma$			
(0–0) + (2–1)	4.1 ± 0.24	-	-
(0–0)	3.1 ± 0.18	-	-
(2–1)	1.0 ± 0.6	-	-

Table 3. Absolute emission cross-section values following 100 eV electron impact onto CH_3F, CH_2F_2 and CHF_3 for the observed CH: $A^2\Delta \rightarrow X^2\Pi$-system, the CH^+: $A^1\Pi \rightarrow X^1\Sigma$-system, the $B^2\Sigma^- \rightarrow X^2\Pi$-system and the Balmer-lines H_α–H_ξ. All values have the unit 10^{-19} cm^2.

Compound	CH_3F	CH_2F_2	CHF_3
Transition			
CH: $A^2\Delta \rightarrow X^2\Pi$			
complete transition	14.75 ± 0.88*	7.094 ± 0.42*	2.171 ± 0.13
(0–0)	7.02 ± 0.42	3.35 ± 0.20	0.91 ± 0.05
(1–1)	6.31 ± 0.38	3.01 ± 0.18	0.81 ± 0.05
(2–2)	1.42 ± 0.08	0.74 ± 0.04	0.45 ± 0.03
CH^+: $A^1\Pi \rightarrow X^1\Sigma$			
(0–0) + (2–1)	3.23 ± 0.19	3.23 ± 0.19	2.01 ± 0.12
(0–0)	2.62 ± 0.16	2.62 ± 0.16	1.63 ± 0.10
(2–1)	0.61 ± 0.04	0.61 ± 0.04	0.38 ± 0.02
CH: $B^2\Sigma^- \rightarrow X^2\Pi$			
(0–0)	8.82 ± 0.61	6.56 ± 0.45	4.20 ± 0.28
Balmer-lines			
H_α	25.73 ± 0.53*	20.59 ± 1.22	16.34 ± 0.97*
H_β	6.72 ± 0.40*	4.95 ± 0.29*	3.56 ± 0.21*
H_γ	3.01 ± 0.18*	2.02 ± 0.12*	1.36 ± 0.08*
H_δ	1.36 ± 0.094*	0.99 ± 0.069	0.82 ± 0.056*
H_ϵ	1.13 ± 0.078*	0.89 ± 0.0622	0.67 ± 0.046
H_ξ	0.60 ± 0.041	0.49 ± 0.034	0.35 ± 0.024

The $B^2\Sigma \rightarrow X^2\Pi$-system of CH which appears between 387 nm and 415 nm is contaminated by the atomic H-lines H_δ, H_ϵ and H_ξ. The analysis of the observed (0–0)-band was again performed by comparing calculated synthetic spectra withe measured emission spectra. The calculated line positions are in a very good agreement with the data of Bernath *et al.* [18]. For rotational quantum numbers up to $J = 13.5$ deviations are less than 0.05 nm. However, the intensity distribution could not be reproduced by a unique thermal population of the rotational states. For higher rotational quantum numbers, there is an increasing difference between the measured and the calculated intensities. But the line intensities could be adjusted by a factor in the exponent of the Boltzmann-factor, which depends on the rotational quantum number. This factor means that the population of the higher rotational states is greater than in thermal equilibrium. A similar non-thermal behaviour has been observed for the (0–0)- and (1–0)-bands of the OH-radical earlier [19,20]. The calculated synthetic spectra and the meausured emission spectra of all investigated target compounds are shown in the Figures 5a–5c. The strongest non-thermal behaviour is observed in the emission spectrum of CH_2F_2 which shows a strong increase of the intensity between 390 nm and 392 nm followed by a steep decrease. Although it was possible to reproduce the intensity distribution for many rotational lines using the correction factor, there still remains a large difference in the broadening of the rotational lines. At higher rotational quantum numbers, the measured emission lines appear to be nearly continuous, whereas the lines in the synthetic spectra yield a discrete structure. The strongest broadening can be observed in the Q-branch with quantum numbers greater than $J = 13.5$. We assume that the reason for this behaviour is the predissociation of the molecules in highly excited rotational levels of the excited electronic state.

Because of the differences between synthetic and measured spectra, it was not possible to calculate absolute emission cross-sections in detail. However, the experimentally determined shapes of the Balmer-lines H_δ–H_ξ could be used for further calculations. By subtracting the values of the Balmer line intensities, the absolute emission cross-sections of the total (0–0)-band of the $B^2\Sigma \rightarrow X^2\Pi$-system for all compounds could be obtained by integrating the remaining intensities over the entire spectral region of the (0–0)-band. These absolute emission cross-sections for $B^2\Sigma \rightarrow X^2\Pi$- and the Balmer-emission, which are listed in Table 3, show again a linear dependence on the number of H-atoms in the target, which was observed for the $A^2\Delta \rightarrow X^2\Pi$-system, whereas the CH^+-system does not show any dependence on the number of H-atoms. The absolute emission cross-sections for $A^2\Delta \rightarrow X^2\Pi$, $B^2\Sigma \rightarrow X^2P$ and H_δ–H_ξ are plotted *versus* the number of H-atoms in Figures 6a–6c. These experimental results give a strong hint, that the increasing cross-section for the production of excited H-atoms by electron impact is merely a steric effect, while the production of excited neutral or ionic radicals is due to more complex processes in the highly excited states of the parent molecule.

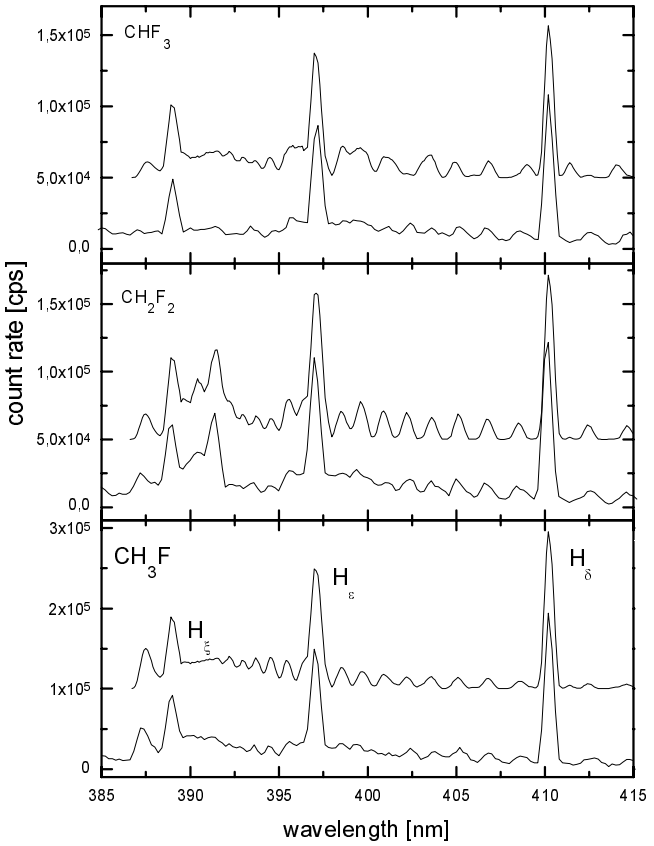

Fig. 5. Convolution of the H_δ–H_ξ-line with the calculated spectrum of CH: $B_2\Sigma \rightarrow X_2\Pi$ (0–0) band, upper curves, measured spectrum, lower curves, for the various compounds.

4.2 The VUV emission spectra

The emission spectra of CH_3F, CH_2F_2, CHF_3 and CF_4 following 100 eV electron impact in the spectral range between 100 nm and 200 nm are shown in the Figure 7. The spectral band pass of the monochromator was $\Delta\lambda = 0.275$ nm fwhm. The emission spectra of CH_3F, CH_2F_2 and CHF_3 show the same atomic lines, but with different relative intensities. There are several C(I)-lines due to singlet and triplet transitions above the Lyman-α-line. The spectra show additionally an atomic C(II)-line. The emission spectrum of CF_4 shows the same atomic C-lines, which now are superimposed on a continuous emission between 150 and 180 nm. Photon/ion-coincidence experiments [21] have shown that the emitter of this continuous part is a highly excited CF_3^+-ion which will be formed by the fast decay of $CF_4^+(X)$. The $CF_4^+(X)$ state will be populated from the $CF_4^+(D)$ state which will be directly formed in the collision process. A similar process leads to the continuous radiation which can be observed between 200 nm and 500 nm in the emission spectrum of CF_4 [2].

Using the data of Möhlmann and de Heer [8] absolute emission cross-sections for the Lyman-α-line were determined for CH_3F, CH_2F_2 and CHF_3 by means of equation (1) and are listed in Table 4. The reported statistical error limits were obtained from repeated measurements of the Lyman-α-line. Figure 6 (lower right part). shows the determined absolute emission cross-sections for Lyman-α emission plotted against the number of H-atoms of the different targets. A linear dependence can be observed again.

Table 4. Absolute emission cross-section values of the Lyman-α-line and of the atomic C-lines at 156.1 nm and 165.7 nm following 100 eV electron impact onto CH_3F, CH_2F_2 and CHF_3. All values have the unit 10^{-19} cm^2.

Compound	CH_3F	CH_2F_2	CHF_3
$\sigma_{abs(100\ \mathrm{eV})}L\alpha$	10.9 ± 0.56	8.2 ± 0.41	5.8 ± 0.30
C: 156.1 nm	3.33 ± 0.26	3.68 ± 0.28	4.84 ± 0.37
C: 165.7 nm	5.75 ± 0.44	5.82 ± 0.45	7.00 ± 0.54

In order to obtain absolute emission cross-sections of the C(I)-lines at 156.1 nm and 165.7 nm the sensitivity of the optical detection system at these wavelengths was determined by means of known absolute emission cross-section data for the (3–2)-, (2–2)-, (3–4)- and (1–3)-bands of the 4th positive system of CO at 154.2 nm, 157.6 nm 164.7 nm and 166.9 nm. The sensitivity at 165.7 nm was obtained by a linear interpolation between the values at 164.7 nm and 166.9 nm, as the sensitivity varies only very weakly in this spectral range. Between 154.2 nm and 157.6 nm there is a stronger variation of the sensitivity, so that a linear as well as a square interpolation was used to determine the sensitivity at 156.1 nm. But the difference between both interpolations was less than 0.5%. The absolute emission cross-sections of both C(I)-lines are listed in Table 4 for all compounds. There is no dependence on the number of H-atoms in the target.

In order to find additional spectral details in the emission spectra the electron energy was increased to 300 eV which yielded an electron current of 400 μA. Also the gas pressure in the gas line was increased to 0.3 mbar, to increase the count rate. Emission spectra of CH_2F_2 and CHF_3 were now recorded again with a spectral resolution of $\Delta\lambda = 0.165$ nm fwhm (CH_2F_2) and $\Delta\lambda = 0.110$ nm fwhm (CHF_3) respectively. Figure 8 for CH_2F_2 and Figure 9 for CHF_3 show the resulting emission spectra. An enlarged plot of the spectral region between 145 nm and 165 nm is inserted and shows that the discrete line at 158 nm is superimposed on an extremely weak continuous structure the maximum of which is at 156 nm. This continuous part cannot be observed in the emission spectrum of CH_3F, but is very similar to the feature in the emission spectrum of F_2 following 106 eV electron impact [22]. The continuous part was assigned to the fluorescence of several emitting excited electronic states of F_2. The assumption that F_2 is the emitter of the weak continuous part in our emission spectra is in agreement with the prediction of Martinez *et al.* [23] and the corresponding excitation functions of the CH and CH^+ systems which showed evidence for the presence of radiation from the excited D'-state of F_2, as mentioned earlier [3].

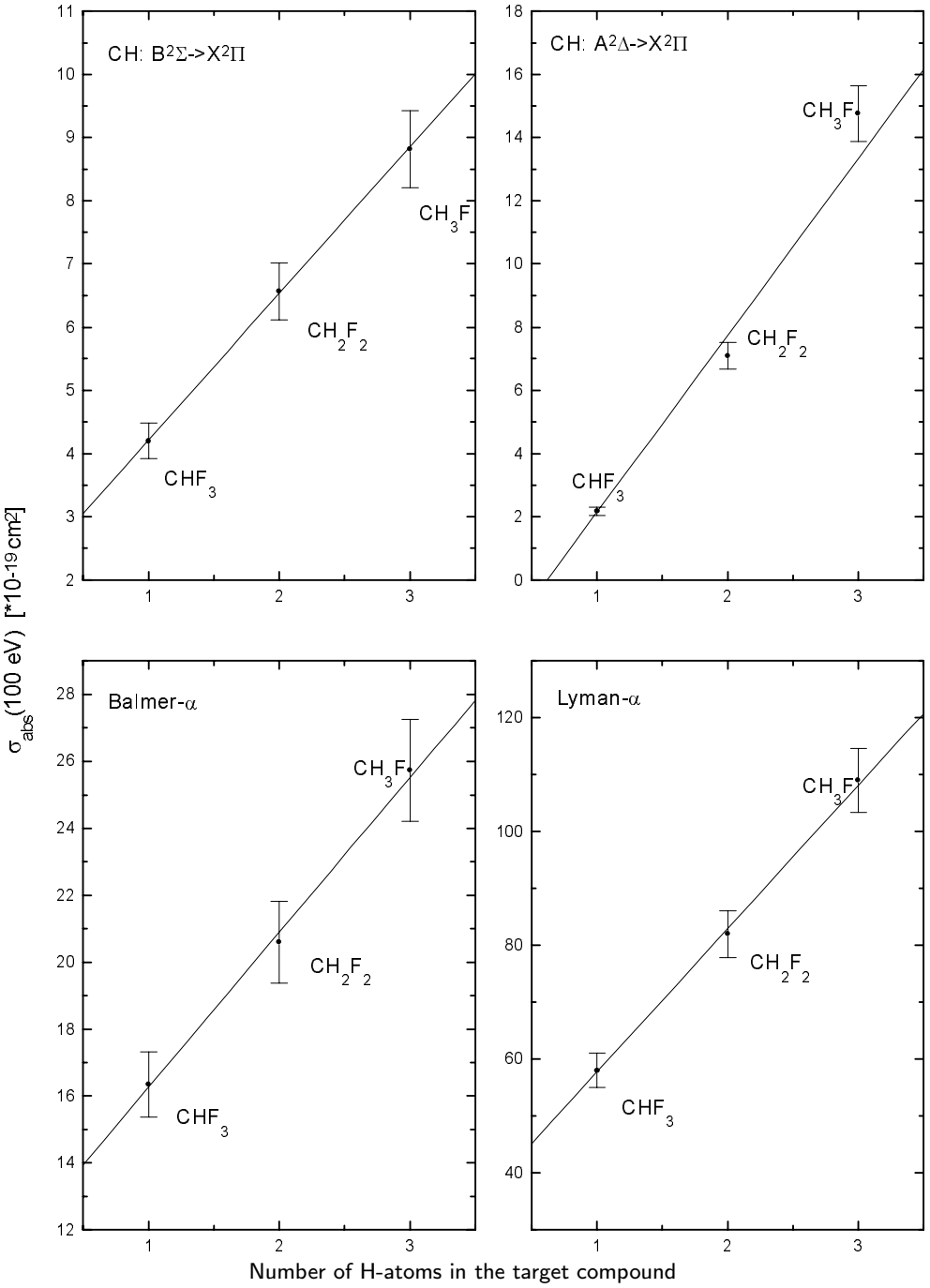

Fig. 6. The linear dependence of the cross-sections of given spectral components on the number of H-atoms in the target molecules.

4.3 Relative emission cross-sections – excitation functions

Figure 10 shows the excitation functions of the C(I)-line at 247.9 nm for CH_3F, CH_2F_2 and CHF_3 recorded with the IRUV-apparatus using the crossed-beam-system. The excitation function for CH_3F as target molecule has a first onset at 19.8 eV. For CH_2F_2 and CHF_3 the excitation functions of this line show several onsets: for CH_2F_2 there is a first one at 8.2 eV and a second one at 12.2 eV. Because the C(I)-line is superimposed on the continuous radiation emitted by excited CF_2, the excitation function contains contributions of this continuous radiation. The onset values are in very good agreement with onset values which were reported for this continuous part earlier [3]. A third onset may be estimated at 27.8 eV and only this onset can be associated with the emission of the C(I)-line. But because the continuous underground influences not only the absolut value, but also the slope of an excitation function, an exact determination of the third onset value requires a more exhaustive analysis of the continous part. A similar behavior can be observed in the excitation function obtained for CHF_3. The onset at 15.2 eV is due to the continuous part in the emission spectrum and

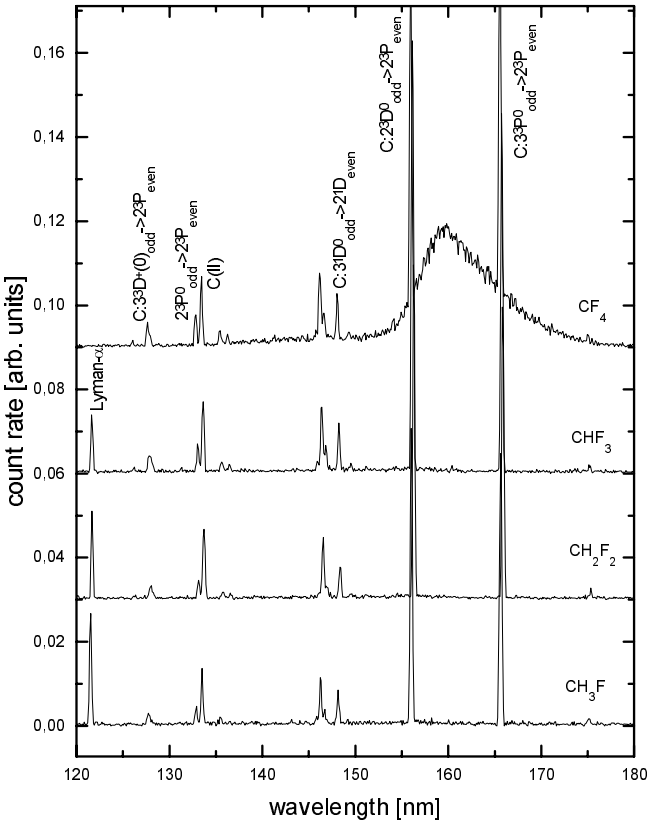

Fig. 7. The main features of the VUV emission spectra of the fluoromethans and for comparison of CF_4. Further explanation in the text.

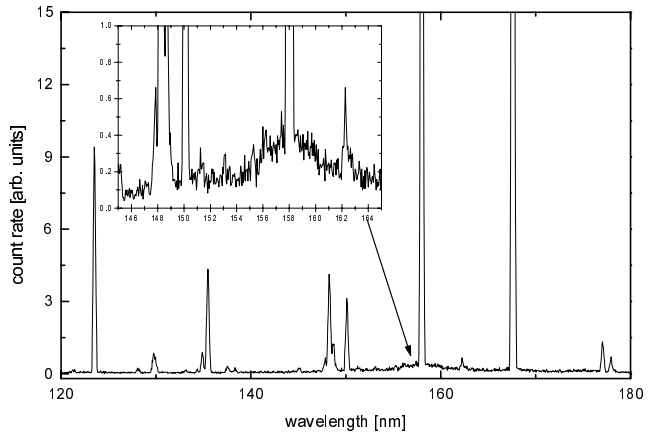

Fig. 8. The VUV emission spectrum of CH_2F_2 as in Figure 7 at enhanced energy of 300 eV shows an additional continuous structure.

a second onset, due to the C(I)-line, appears at 27.8 eV. Because the atomic C(I)-line in the continous part of the CH_4 spectrum is only very weak its excitation function has not been recorded.

Figure 11 shows the correponding Fano-plots of the excitations functions. From the linear slope in the high energy region one concludes, that only optical allowed processes lead to the emission of the C(I)-line in the spectra of CH_2F_2, CHF_3 and CF_4, wheras the Fano-plot of CH_3F consist of two parts. A linear part above the threshold is followed by a nearly horizontal slope in the high energy region (*e.g.* $\log E > 2.7$) which indicates the presence of a second, optically forbidden dissociative channel.

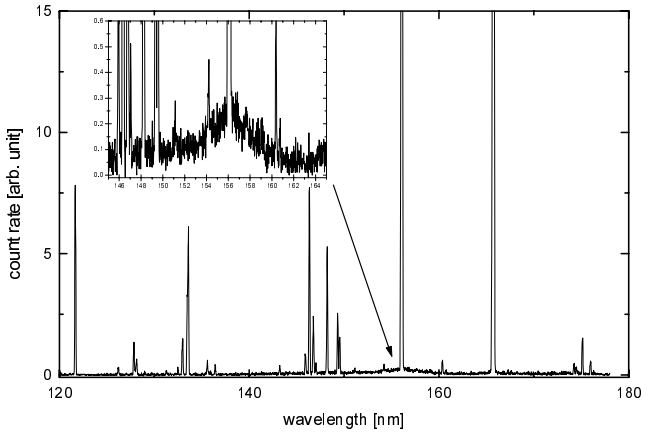

Fig. 9. The VUV emission spectrum of CHF_3 as in Figure 7 at enhanced energy of 300 eV shows an additional continuous structure too.

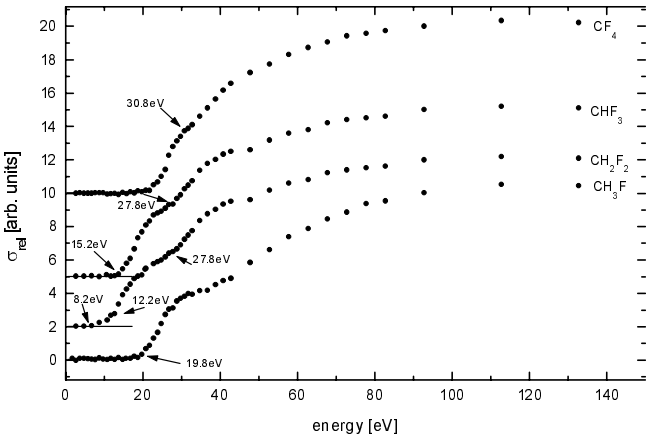

Fig. 10. Excitation functions of the C(I)-line at 247.9 nm for all investigated compounds with characteristic onsets. Explanation in text.

Because both C-lines at 247.9 nm and 192 nm have their origin in the same excited 3^1P-state they can be observed for all compounds simultaneously and must show the same energetic threshold value in the corresponding excitation functions. Because the atomic C(I)-line at 192 nm is isolated in the emission spectra of all fluoromethanes it is possible to determine the threshold value for the formation of excited C(I). The observed onset values in Figure 12 are exclusively due to the C(I)-line. It was also possible to record an unperturbed excitation function of the C(I)-line in the emission spectrum of CF_4. The onset values for CH_2F_2, CHF_3 and CF_4 are in a similar energy range of 24.8 eV, 25.2 eV and 25.8 eV which is about 2–3 eV lower than the estimated onset values

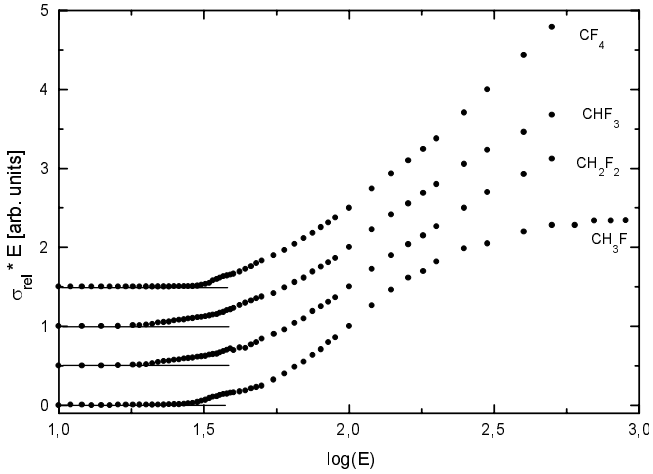

Fig. 11. Fano-plots of the excitation-functions from Figure 10.

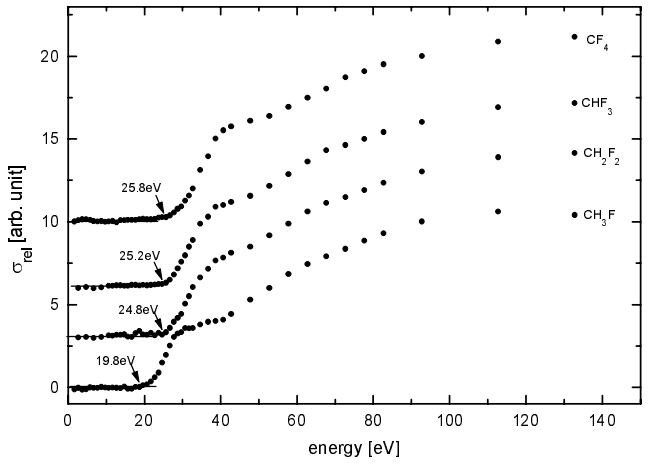

Fig. 12. Excitation functions of the C(I)-line at 193.1 nm for all investigated compounds with characteristic onsets. Explanation in text.

Table 5. Threshold values of the excitation functions observed for the C-lines at 193.1 nm and 247.9 nm and of the Lyman-α excitation functions following electron impact onto the target compounds. The experimental uncertenity of the electron energy is ± 1.5 eV.

Compound wavelength	CH_3	CH_2F_2	CHF_3	CF_4
C: 193.1 nm	19.8 eV	24.8 eV	25.2 eV	25.8 eV
C: 247.6 nm	19.8 eV	19.8 eV	21.8 eV	21.8 eV
Lyman α	21.2 eV	22.3 eV	21.5 eV	-

of the line at 247.9 nm while the onset in the excitation function of CH_3F at 19.8 eV is the same as for the C(I) line at 247.9 nm. All onset values for the C(I)-lines are listed in Table 5. Figure 13 shows again the corresponding Fano-plots which are very similar to the Fano-plots in Figure 11. For CH_3F there are again two parts from optically allowed and forbidden dissociative processes whereas the

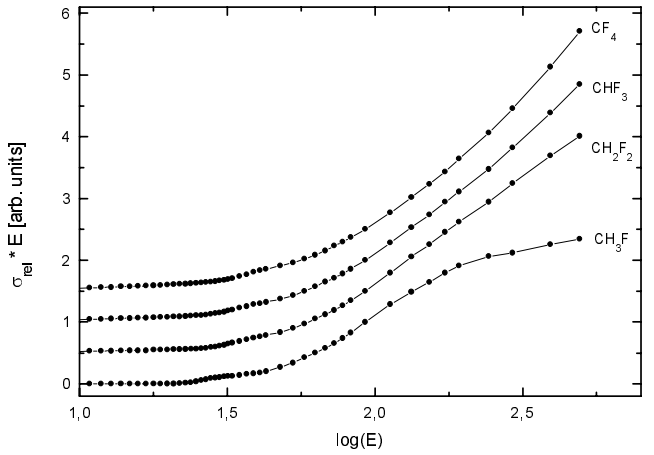

Fig. 13. Fano-plots corresponding to the excitation-functions from Figure 12.

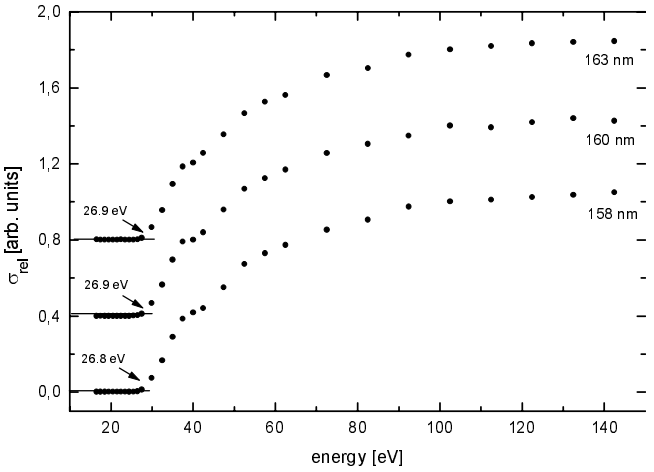

Fig. 14. Excitation function of the continuous part of the VUV emission of CF_4 at various wavelength.

Fano-Plots of the other targets show only optically allowed transitions. For CH_3F we find the most probable process:

$$CH_3F \rightarrow C(3^1P) + H_2 + H + F \qquad (\Delta H_{calc} = 20.5 \text{ eV}). \quad (2)$$

The calculated minimum value of ΔH lies 0.7 eV above the measured onset values. This difference can be explained by the uncertainity in the electron energy of about 1 eV.

The excitation functions of the Lyman-α-line following electron impact on CH_3F, CH_2F_2 and CHF_3 were determined using the crossed-beam-system in the VUV-apparatus. Onset values are listed in Table 5. Within the uncertainity of the electron energy all values are the same as those reported for the Balmer-emissions in the visible part of the emission spectra [3]. Therefore, it must be concluded, that the first excited state becomes populated only by cascading from higher excited states. A direct population of the first excited state could not be observed.

Excitation functions were also measured for the C(I)-line at 133.5 nm and the atomic C-lines at 148.2 nm

Table 6. Threshold values of the excitation functions observed for the C-lines and the C(I)- line following electron impact onto the target compounds. The experimental uncertenity of the electron energy is ± 1.5 eV.

Transition	C(I) 133 nm	C 148.2 nm	C 156.1 nm	C 165.7 nm
Compound		singulet	triplet	triplet
CH_3F	31.8 eV	29.5 eV	27.7 eV	27.5 eV
CH_2F_2	37.5 eV	30.0 eV	28.5 eV	29.7 eV
CHF_3	38.1 eV	32.5 eV	31.9 eV	31.8 eV
CF_4	30.0 eV	27.8 eV	27.1 eV	27.8 eV

Table 7. Threshold values of the excitation functions observed for the continuous part of the VUV emission spectrum of CF_4. The experimental uncertenity of the electron energy is ± 1.5 eV.

Wavelength	Threshold	Onset
158 nm	26.8 eV	40.0 eV
160 nm	26.9 eV	40.0 eV
163 nm	26.9 eV	40.0 eV

(singlet) 156.1 nm (triplet) and 165.7 nm (triplet). The corresponding threshold values are listed in Table 6. All excitation functions show a very slow increase up to the maximum value at about 140 eV. Observations at even higher energies for obtaining Fano-plots were not possible in the VUV-apparatus.

The excitation functions of the atomic C-lines show a second onset above 50 eV. These threshold values are higher than calculated thermochemical data, so it must be assumed that the formation of excited C-fragments follows the dissociation from highly excited Rydberg-states of the target molecule which cannot be populated by optically allowed transitions. A similar behavior was observed by Allcock and McConkey for the formation of atomic F-fragments following electron impact on CHF_3 [24], which means that highly excited target molecules dissociate into atomic fragments. Because the threshold values are in the same region as the observed second onset of the excitation functions of the Balmer-lines, we assume a second dissociative channel which leads to the formation of highly excited C- and H-fragments.

The excitation functions of the continuous part in the VUV emission spectrum of CF_4 are presented in Figure 14 for several wavelengths. Threshold energies and second onset values are listed in Table 7. The threshold energies are about 3.3–3.4 eV higher than the threshold values of the continuous part between 200 nm and 500 nm in the emission spectrum of CF_4. Müller *et al.* [2] explained the continuous part between 200 nm and 500 nm by the formation of CF_4^+ into the excited C-state which rapidly decays into its ground state. From this state the CF_4^+-ion dissociates into CF_3^+ and atomic F. But since the energetic difference of the onset values is equal to the energetic distance of corresponding points in the continua, *i.e.* the maxima of both continua, the higher onset values of the excitation functions for the continuous part in the VUV spectral region can be explained by the formation of CF_4^+ in the excited D-state. For both continua the emitting source should be an excited state of CF_4^+.

5 Conclusion

The emission spectra of the fluoromethanes following 100 eV electron impact have been invetigated in the spectral range between 100 nm and 700 nm. Absolute emission cross-sections were calculated directly from the calibration data and the measured spectra using the IRUV-apparatus. In the VUV spectral region, absolute emission cross-sections for some atomic lines were obtained relative to known cross-sections of atomic lines and molecular band systems.

Data for the dynamic viscosity of the fluoromethanes have been controlled by measuring the gaspressures under molecular flow conditions and lead to nearly perfect agreement with known values of cross-sections, but required a revision of previously reported values of emission cross-sections. Absolute emission cross-section were determined for the $A^2\Delta \rightarrow X^2\Pi$-system of CH and the $A^1\Pi \rightarrow X^1\Sigma^+$-system of CH^+ by means of synthetic emission spectra. This procedure allowed the determination of cross-section values for several vibronic band systems for all H-atom containing compounds. The absolute emission cross-section of atomic lines of the Balmer-series were obtained directly form the measured emission spectra. The cross-section values for the $B^2\Sigma \rightarrow X^2P$-system of CH were calculated from the measured emission spectra relative to the cross-section values of the atomic Balmer-lines which are superimposed on the $B^2\Sigma \rightarrow X^2P$-system. Because of the strong non-thermal behaviour of this system and the broadening of the rotational lines due to predissociation, this band system could not be analyzed from synthetic spectra. The absolute emission cross-sections of CH-band systems and of the Balmer-lines show a linear dependence on the number of H-atoms in the target whereas the observed CH^+-system does not show this behaviour.

The emission spectra following 100 eV electron impact of the fluoromethanes as well as relative emission cross-sections of spectral components in the VUV spectral region between 100 nm and 200 nm were analysed by means of crossed beams in the VUV-apparatus. The strongest components of the emission spectra are atomic C-lines and

the Lyman-α-line for H-atom containing compounds. Only the spectrum of CF_4 shows a continuous part between 150 nm and 180 nm. Absolute emission cross-sections of the Lyman-α-line and two atomic C-lines were obtained relative to the well-known absolute emission cross-sections of some diatomic band systems and atomic lines. The values for the Lyman-α-line show again a linear dependence on the number of H-atoms in the target whereas the values of the C-lines do not show this behaviour.

A more detailed analysis of the emission spectra of CH_3F, CH_2F_2 and CHF_3 showed the appearance of a very weak continuous part between 145 nm and 165 nm which could not be observed in the emission spectrum of CH_3F. This continuous part is very similar to the continuous part in the emission spectrum of F_2 following 106 eV electron impact [19]. According to the prediction of Martinez *et al.* [23], which is in good agreement with the analysis of relative emission cross-section of several CH-systems [3], we assign the continuous emission to transitions from the excited D'-state of F_2. The very weak intensity can be explained by the long lifetimes of the excited species. Similar to the LBH-system of N_2, excited fragments leave the observed collision volume before radiating.

In addition to the relative emission cross-section reported earlier [3], new excitation functions of spectral components in the VUV region were analysed. A detailed analysis of the excitation functions of the two atomic C-lines at 247.9 nm and 192 nm shows that the dissociation channels for CH_3F are different from those of the other fluoromethanes.

Evidently two different dissociation mechanisms lead to the formation of atomic fragments. In one case, we found atomic fragments which follow higly excited stats in the target molecules and in the other case merely steric effects support the removal of single excited H-atoms during the dissociation process.

The excitation functions of the continuous part between between 150 nm and 180 nm in the VUV emission spectrum of CF_4 show first onsets which are about 3.3–3.4 eV higher than the first onsets in the excitation functions of the continuous part between 200 nm and 500 nm. This ernergetic difference is in good agreement with the difference between both maxima of the continuous parts and gives some evidence that the emitter of both continua is an excited state of CF_4^+.

We gratefully acknowledge helpful discussions with Prof. Kurt H. Becker of the Stevens Institute of Technology, Hoboken, NJ 07030, Department of Physics and Engineering Physics. We also want to thank Prof. J.W. McConkey, University of Windsor, Department of Physics, for helpful and encouraging discussions.

References

1. U. Müller, G. Schulz, J. Chem. Phys. **96**, 5924 (1992).
2. U. Müller, Th. Bubel, G. Schulz, A. Sevilla, J. Dyke, K. Becker, Z. Phys. D **24**, 131 (1992).
3. O. Keller, C. Mang, M.U. Nikola, G. Schulz, Z. Phys. D **37**, 315 (1996).
4. Landolt-Börnstein: II. Bd, 5. Teil, Nr. 251113 (Springer-Verlag, Berlin-Heidelberg-New York, 1968), pp. 44–57; D'Ans. Lax: I. Bd., Nr. 71132 (Springer-Verlag, Berlin-Heidelberg-New York, 1983), p. 1424.
5. H.A. van Sprang, H.H. Brongersma, F.J. De Heer, Chem. Phys. Lett. **65**, 55 (1979).
6. G.R. Möhlmann, K.H. Shima, F.J. De Heer, Chem. Phys. **28**, 331 (1978).
7. J.F.M. Aarts, C.I.M. Beenakker, F.J. De Heer, Physica **53**, 32 (1971).
8. G.R. Möhlmann, F.J. De Heer, Chem. Phys. **19**, 233 (1977).
9. M.J. Mumma, E.J. Stone, E.C. Zipf, J. Chem. Phys. **54**, 2627 (1971).
10. W. Lichten, J. Chem. Phys. **26**, 306 (1957).
11. J. Olmstead, A.S. Newton, K. Street, J. Chem. Phys. **42**, 2321 (1965).
12. R.F. Holland, J. Chem. Phys. **51**, 3940 (1969).
13. G. Herzberg, *Molecular Spectra and Molecular Structure I., Spectra of diatomic molecules* (van Nostrand Reinhold, New York, 1950).
14. A. Carrington, D.A. Ramsay, Phys. Scripta **25**, 272 (1982).
15. B.H. Mahan, A. O'Keefe, Chem. Phys. **69**, 35 (1982).
16. L.T. Earls, Phys. Rev. **48**, 423 (1935).
17. S. Waldenstroem, K.R. Nagvi, J. Chem. Phys. **87**, 3563 (1987).
18. P.F. Bernath, C.R. Brazier, T. Olsen, R. Hailey, W.T.M.L. Fernando, J. Mol. Spectr. **147**, 16 (1991).
19. U. Müller, Th. Bubel, G. Schulz, Z. Phys. D **25**, 167 (1993).
20. T. Carrington, J. Chem Phys. **60**, 3707 (1974).
21. U. Müller, M. Lange, W. Haas, R. Brenn, J. Chem. Phys. **100**, 5550 (1994).
22. D. Spence, H. Tanaka, M.A. Dillon, K. Lanik, J. Phys. B: At. Mol. Phys. **19**, L569 (1986).
23. R. Martinez, F. Castano, M.N. Sanchez Rayo, R. Pereira, Chem. Phys. **172**, 349 (1993).
24. C. Allock, J.W. McConkey, J. Phys. B **11**, 741 (1978).